Structural investigation of the molybdenum site of the periplasmic nitrate reductase from *Thiosphaera pantotropha* by X-ray absorption spectroscopy

Brian BENNETT*¶, John M. CHARNOCK†‡, Heather J. SEARS§, Ben C. BERKS§, Andrew J. THOMSON*, Stuart J. FERGUSON‖, C. David GARNER‡ and David J. RICHARDSON§**

Centre for Metalloprotein Spectroscopy and Biology, Schools of *Chemical and §Biological Sciences, University of East Anglia, University Plain, Norwich NR4 7TJ, †C.L.R.C. Daresbury Laboratory, Warrington, Cheshire WA4 4AD, ‡Department of Chemistry, University of Manchester, Manchester M13 9PL, and ‖Department of Biochemistry, University of Oxford, South Parks Road, Oxford OX1 3QU, U.K.

The molybdenum centre of the periplasmic respiratory nitrate reductase from the denitrifying bacterium *Thiosphaera pantotropha* has been probed using molybdenum K-edge X-ray absorption spectroscopy. The optimum fit of the Mo(VI) EXAFS suggests two =O, three –S– and either a fourth –S– or an –O–/–N– as molybdenum ligands in the ferricyanide-oxidized enzyme. Three of the –S– ligands are proposed to be the two sulphur atoms of the molybdopterin dithiolene group and Cys-181. Comparison of the EXAFS of the ferricyanide-oxidized enzyme with that of a nitrate-treated sample containing 30% Mo(V) suggests that the Mo(VI) → Mo(V) reduction is accompanied by conversion of one =O to –O–. The best fit to the Mo(IV) EXAFS of dithionite-reduced enzyme was obtained using one =O, one –O– and four –S–/–Cl ligands. The periplasmic nitrate reductase molybdenum co-ordination environment in both the Mo(VI) and Mo(IV) oxidation states is distinct from that found in the membrane-bound respiratory nitrate reductase.

INTRODUCTION

Molybdenum-containing enzymes are found in all forms of life from bacteria to higher plants and humans [1]. With the exception of the molybdenum nitrogenases, which bind a molybdenum-iron sulphur cofactor [2,3], all molybdenum enzymes contain one of a series of pterin–molybdenum cofactors based on a pterin–pyran tricycle (molybdopterin) [4–6]. A dithiolene group on the pyran ring provides bidentate sulphur ligation of the molybdenum atom.

Three distinct types of nitrate reductase, all containing a GMP conjugate of the molybdopterin cofactor (molybdopterin guanine dinucleotide; MGD), have been identified in bacteria [7]. Membrane-bound respiratory nitrate reductases [7–12] are involved in energy-conserving anaerobic electron-transport pathways. They are $\alpha\beta\gamma$ heterotrimers in which the MGD cofactor is bound by the α subunit. Four [Fe–S] clusters are bound by the β subunit [12,13], and two *b*-type haem groups are bound by the integral membrane quinol-oxidizing γ subunit [13]. The periplasmic respiratory nitrate reductases are water-soluble heterodimers of an MGD- and 1 × [4Fe–4S]-containing subunit and a *c*-type cytochrome [7,14–17]. Assimilatory nitrate reductases are water-soluble monomeric cytoplasmic enzymes binding MGD and one or more [Fe–S] clusters [7,18]. A combination of primary structure analysis and Mo(V) EPR spectroscopy suggests that the molybdenum environments in the two water-soluble bacterial nitrate reductases are similar to each other but distinct from that in the membrane-bound nitrate reductase [7,16–18].

The periplasmic nitrate reductase of *Thiosphaera pantotropha* exhibits multiple Mo(V) EPR signals, of which the one denoted High-*g* Split is thought to be catalytically and physiologically relevant [16,19]. It was proposed that Mo(V) in this species has two –S– ligands arising from the cofactor dithiolene moiety and a third from a conserved Cys-181. The lack of either a Mo–OH or Mo–SH ligand was suggested by the lack of coupling of Mo(V) to a solvent-exchangeable proton. The presence of the cysteine-derived –S– ligand was suggested by the nature of the EPR signals of the dithionite-reduced enzyme [16]. The identity of further Mo ligands could not be ascertained from Mo(V) EPR spectroscopy. To obtain direct information regarding the ligand sphere of the molybdenum atom of the periplasmic nitrate reductase of *T. pantotropha* a molybdenum K-edge X-ray absorption spectroscopic (XAS) study has been undertaken.

EXPERIMENTAL

Nitrate reductase was purified as described previously [14] from periplasmic extracts of *T. pantotropha* strain M-6 (*narH*::Tn*5* [Km^r]; [20]). The molybdenum content and catalytic activity of the enzyme as prepared were similar to earlier peparations [14,16]. All reagents used were of A.C.S. or AnalaR quality. Exchange of enzyme into buffer was carried out by exhaustive dialysis in solutions of buffer salts prepared in AnalaR grade water (Fisons). pH electrodes were thoroughly rinsed with AnalaR water and, where KCl was not added, carefully dried with tissue before use to minimize any chloride anion transfer across the glass membrane.

Oxidation of enzyme samples for XAS was effected either by incubation with 10 mM KNO_3 or by additions of $K_3Fe(CN)_6$. The $K_3Fe(CN)_6$ was added to the enzyme as an equal volume of 2 mM $K_3Fe(CN)_6$ in buffer, and the enzyme was reconcentrated by ultrafiltration (Centricon; Amicon). The process was repeated until the optical absorption of the ferricyanide-containing ultrafiltrate indicated that the enzyme had ceased to consume it. Reduction of the enzyme was effected using 10 mM $Na_2S_2O_4$. The nitrate-oxidized and dithionite-reduced samples were prepared in 50 mM Hepes/KOH, pH 7.4, containing 100 mM KCl. The ferricyanide-oxidized sample was prepared in the same buffer in the absence of added chloride. The Mo(V) contents of

Abbreviations used: MGD, molybdopterin guanine dinucleotide; XAS, X-ray absorption spectroscopy.

¶ Present address: Department of Chemistry and Biochemistry, Utah State University, Logan, UT 84322, U.S.A.
** To whom correspondence should be addressed.

samples for XAS were determined by double integration of their EPR spectra and compared with those of a Cu–EDTA standard as in earlier work [16].

Molybdenum K-edge X-ray fluorescence spectra were recorded on frozen solutions at ~ 77 K on the 5T-wiggler magnet beamline, station 9.2 of the Synchrotron Radiation Source, Daresbury Laboratory, operating at 2 GeV with an average current of 150 mA. An Si(220) double crystal monochromator was used, with the second crystal offset to reject 50 % of the beam in order to minimize harmonic contamination. The fluorescence was monitored using a liquid-nitrogen-cooled solid-state thirteen-element Canberra detector. The monochromator was calibrated at the start of the run using a Mo foil, setting the position of the first peak of the derivative of the foil edge to 20002 eV. During multiple scanning of each sample the edge position did not vary. Each spectrum was collected over ~ 45 min with 25, 35 and 50 scans being recorded and summed for the ferricyanide-oxidized, nitrate-oxidized and dithionite-reduced samples respectively.

The raw data were summed using the Daresbury program EXCALIB, and background subtraction was performed using EXBACK. The isolated k^3-weighted EXAFS data were analysed using EXCURV92 [21], employing the single scattering spherical wave approximation [22,23]. Phaseshifts were derived from *ab initio* calculations using Hedin–Lundqvist potentials and von Bart ground states [24]. The theoretical fits were obtained by adding shells of backscattering atoms around the central absorber atom and iterating the absorber-scatterer distances, r, the Debye–Waller type factors, $2\delta^2$, and the Fermi energy correction, E_f, to get the best agreement with the experimental data.

RESULTS

Enzyme samples

The concentration of molybdenum centres in the samples was 0.4 mM in the ferricyanide-oxidized sample and 0.07 mM in the nitrate-treated and dithionite-reduced samples. EPR analysis of the samples indicated that the ferricyanide-oxidized and dithionite-reduced samples each contained < 5 % of the molybdenum as Mo(V). These samples were therefore essentially homogeneous in Mo(VI) and Mo(IV) respectively. As in earlier work [16], the Mo(V) content of the nitrate-treated sample was ~ 30 %. Nevertheless, it would be expected that any Mo(IV) originally present in the sample would undergo turnover-linked oxidation so that the remaining ~ 70 % of the molydenum was present as Mo(VI) [16]. The very small Mo(V) EPR absorption of the dithionite-reduced sample was estimated to be due to approximately equimolar amounts of the High-g Split signal and a second signal denoted Pseudo Rapid Unsplit [16].

EXAFS of ferricyanide-oxidized nitrate reductase

The fits of the ferricyanide-oxidized nitrate reductase EXAFS to a number of models are compared in Table 1. The best fits were obtained assuming a co-ordination number of six. All of the data were fitted using scattering from atoms in the inner co-ordination sphere only (Mo=O, Mo=S, Mo–O– and Mo–S–). Although there is some evidence in the Fourier transforms for shells at ~ 4 Å and at ~ 4.8 Å, attempts to model these with light atom backscatterers (for instance, C atoms in the cofactor) did not improve the fit sufficiently to justify the additional parameters and so were not included in the final fits. The best models are those with two Mo=O bonds at a distance of 1.73 Å. The best fits obtained for this species suggested two =O, three –S– and either a fourth –S–, –O– or –N– ligand. It should be noted here that EXAFS alone does not distinguish between oxygen and nitrogen atoms nor between sulphur and chlorine atoms. This sample was prepared in the strict absence of chloride, making it unlikely that there is any bound chloride. The data and fit with two =O and four –S– ligands are shown in Figure 1(a). The fit for the alternative with three –S– and one –O–/–N– ligand gave a very slightly lower residual, R, implying a similar-quality fit, but was indistinguishable by eye and, hence, is not shown. Reasonable fits could not be obtained (see Table 1) for models with only one oxo ligand (Figure 1b) or with an =O and a =S

Table 1 EXAFS residual *R* factors for various model fits

n is the number of scatterers in each shell, *r* is the absorber atom-scatterer distance, and $2\delta^2$ is the Debye–Waller factor.

	Mo=O			Mo=S			Mo–O			Mo–S			
Sample treatment	*n*	*r* (Å)	$2\delta^2$ (Å^2)	*n*	*r* (Å)	$2\delta^2$ (Å^2)	*n*	*r* (Å)	$2\delta^2$ (Å^2)	*n*	*r* (Å)	$2\delta^2$ (Å^2)	Residual
$K_3Fe(CN)_6$ (Figure 1a)	2	1.73	0.002	–	–	–	–	–	–	4	2.43	0.014	33.4
$K_3Fe(CN)_6$	2	1.74	0.002	–	–	–	1	2.18	0.008	3	2.44	0.011	33.2
$K_3Fe(CN)_6$ (Figure 1b)	1	1.75	−0.003	–	–	–	2	2.27	0.015	3	2.46	0.015	48.1
$K_3Fe(CN)_6$ (Figure 1c)	1	1.72	−0.006	1	2.00	0.005	1	2.30	0.021	3	2.44	0.012	46.4
$K_3Fe(CN)_6$ (Figure 1d)	3	1.73	0.008	–	–	–	–	–	–	3	2.42	0.010	39.8
$K_3Fe(CN)_6$	1	1.73	−0.001	–	–	–	–	–	–	5	2.43	0.019	55.2
$K_3Fe(CN)_6$	2	1.73	0.001	–	–	–	–	–	–	5	2.42	0.018	46.3
NO_3^-	1.8	1.73	0.015	–	–	–	1.1	2.13	0.003	3	2.39	0.005	58.4
NO_3^- (Figure 2b)	2	1.73	0.017	–	–	–	1	2.13	0.002	3	2.40	0.005	59.0
NO_3^- (Figure 2a)	2	1.71	0.015	–	–	–	–	–	–	4	2.38	0.009	60.7
NO_3^-	3	1.71	0.027	–	–	–	–	–	–	3	2.37	0.006	66.6
NO_3^- (Figure 2c)	1	1.73	0.006	–	–	–	2	2.18	0.004	3	2.41	0.009	59.3
NO_3^- (Figure 2d)	2	1.75	0.018	–	–	–	2	2.15	0.002	2	2.42	0.003	59.2
NO_3^-	1	1.71	0.006	–	–	–	–	–	–	5	2.39	0.012	61.4
NO_3^-	2	1.71	0.014	–	–	–	–	–	–	5	2.38	0.012	61.1
$S_2O_4^{2-}$ (Figure 3)	1	1.74	0.008	–	–	–	1	2.06	0.006	4	2.33	0.002	36.6
$S_2O_4^{2-}$	1	1.77	0.008	–	–	–	2	2.09	0.002	3	2.35	0.000	37.7
$S_2O_4^{2-}$	2	1.77	0.029	–	–	–	1	2.06	0.001	3	2.33	0.000	40.0
$S_2O_4^{2-}$	1	1.74	0.010	–	–	–	–	–	–	5	2.31	0.003	40.3

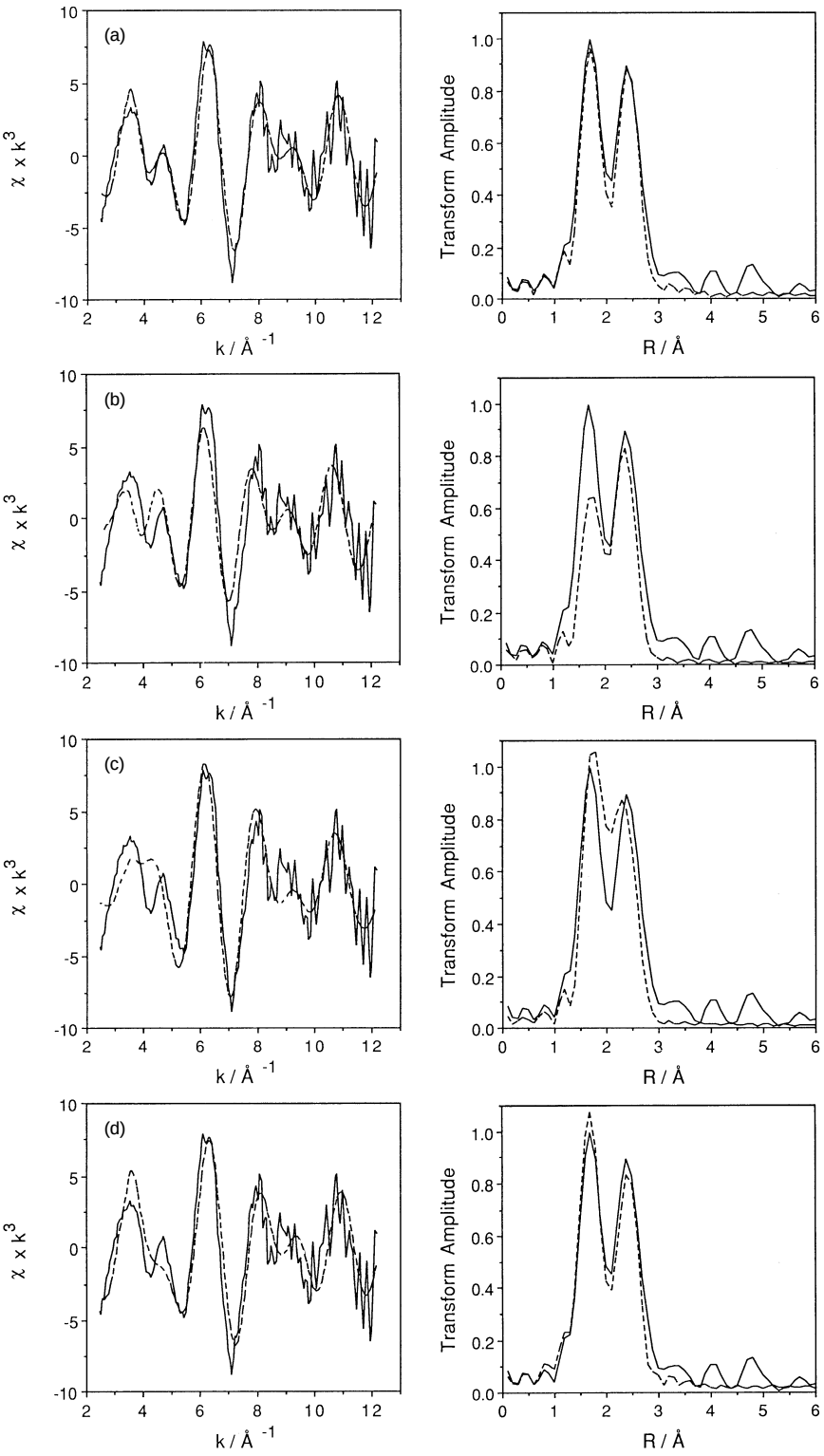

Figure 1 k^3-Weighted EXAFS (left panels) and Fourier transform (right panels) of the molybdenum centre of ferricyanide-treated nitrate reductase

(**a**) The calculated fit assumes two Mo═O and four Mo–S ligands (Table 1). (**b**) The calculated fit assumes one Mo═O, two Mo–O and three Mo–S ligands (Table 1). (**c**) The calculated fit assumes one Mo═S, one Mo═O, one Mo–O and three Mo–S ligands (Table 1). (**d**) The calculated fit assumes three Mo═O and three Mo–S ligands (Table 1). In each graph the solid lines are the experimental data and the dashed lines are the calculated simulations.

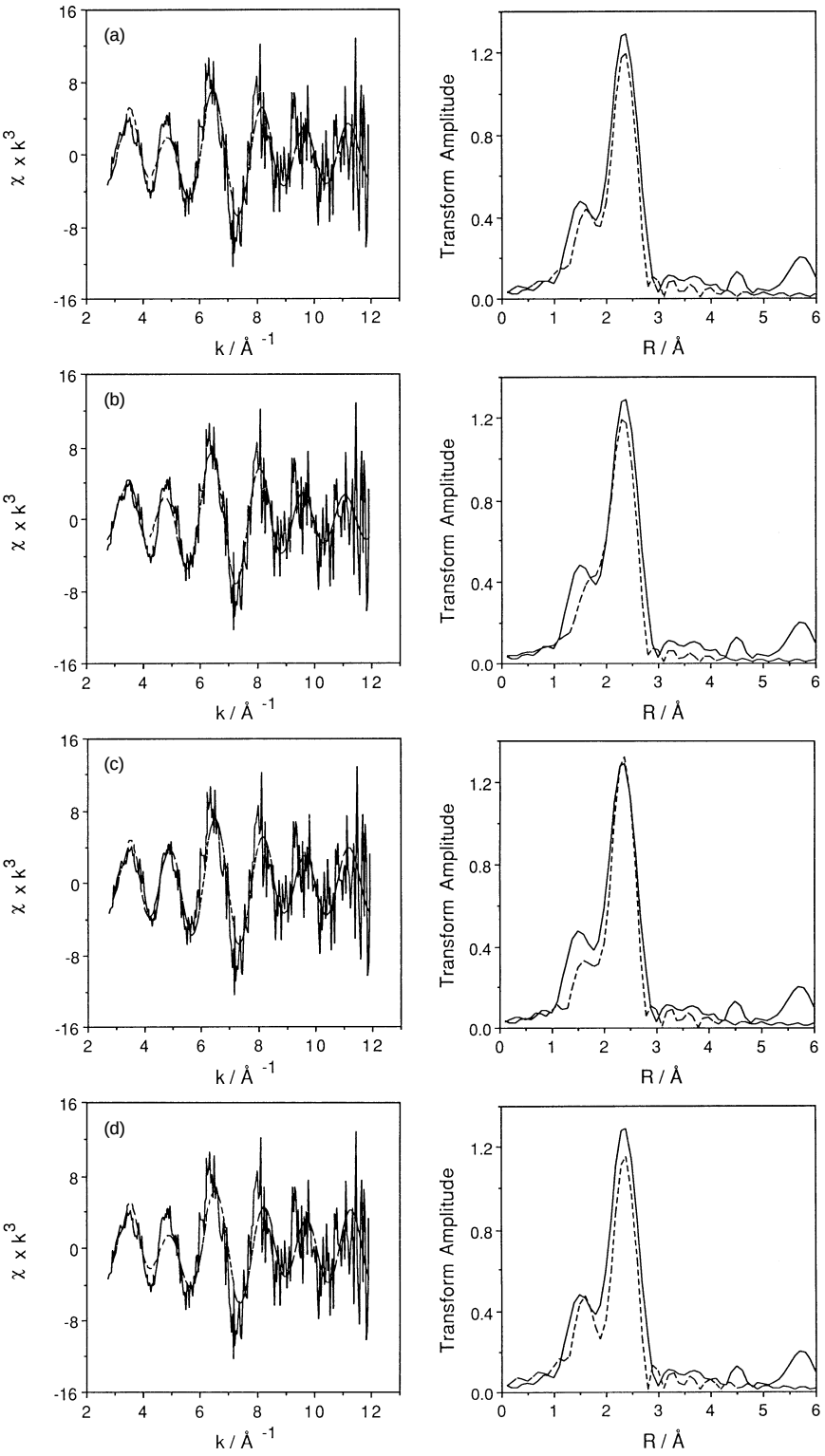

Figure 2 k^3**-Weighted EXAFS (left panels) and Fourier transform (right panels) of the molybdenum centre of nitrate-treated nitrate reductase**

(**a**) The calculated fit assumes two Mo═O and four Mo–S ligands (Table 1). (**b**) The calculated fit assumes two Mo═O, one Mo–O and three Mo–S ligands (Table 1). (**c**) The calculated fit assumes one Mo═O, two Mo–O and three Mo–S ligands (Table 1). (**d**) The calculated fit assumes two Mo═O, two Mo–O and two Mo–S ligands (Table 1). In each graph the solid lines are the experimental data and the dashed lines are the calculated simulations.

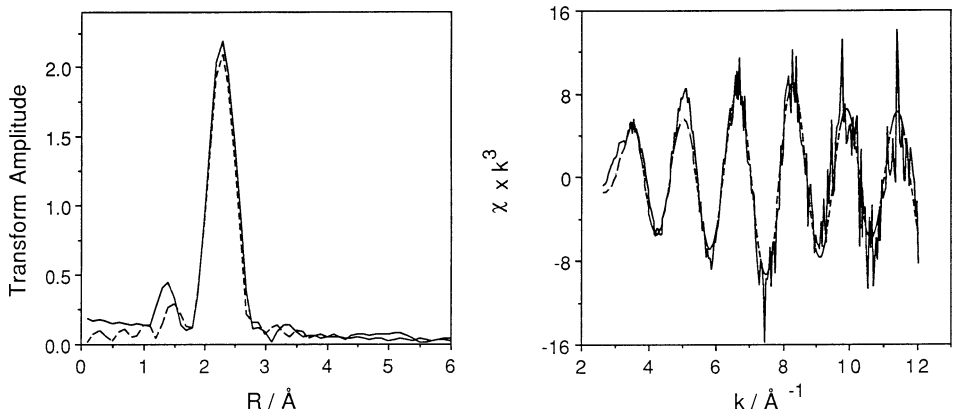

Figure 3 k^3-Weighted EXAFS (right panel) and Fourier transform (left panel) of the molybdenum centre of dithionite-treated nitrate reductase

The calculated fit assumes one Mo=O, one Mo–O and four Mo–S ligands (Table 1). The solid lines are the experimental data and the dashed lines are the calculated simulations.

(Figure 1c), regardless of whatever shells of backscatterers at > 2.1 Å were included. A reasonable fit could not be obtained by assuming three =O and three –S– ligands, one =O and five –S– ligands, or two =O and five –S– ligands.

EXAFS of nitrate-treated nitrate reductase

Some models for the molybdenum co-ordination sphere in nitrate-treated nitrate reductase are given in Table 1, along with their *R* values. The quality of the data from this sample is inferior to that of the data from the ferricyanide-oxidized enzyme because of the lower enzyme concentration. The data quality may also be a reflection of the inhomogeneity of the nitrate-treated sample, in which 30% of the molybdenum is in the Mo(V) state. Various simulations (see Table 1 and Figure 2 for some examples) suggested that nitrate-oxidized nitrate reductase contains one or two Mo=O groups, and approx. three S-donor ligands. The optimum simulation obtained (Table 1) involved 1.8 =O groups at 1.73 Å, 1.1 –O–/–N– atoms at 2.13 Å and 3 –S–/–Cl atoms at 2.39 Å. However, the relatively poor quality of the data requires that the optimum fit is treated with some caution, especially in respect of the occupation number of the shells and the identity of the ligands at 2.13 Å (–O– or –N–) and 2.39 Å (2 –S–/–Cl or 3 –S–).

EXAFS of dithionite-reduced nitrate reductase

The best fit (Table 1; Figure 3) for the Mo(IV) centre of dithionite-reduced nitrate reductase is with one =O, one –O– and four –S–/–Cl ligands. The data could not be satisfactorily fitted assuming two oxo groups (Table 1): the fit was significantly worse, and a high Debye–Waller factor (0.029) was needed for the two =O ligands to obtain even this fit. The data could be fitted quite well to a model with one =O, two –O–/–N– and three –S–/–Cl ligands (Table 1), but a satisfactory fit could not be obtained with less than three –S–/–Cl ligands or with one oxo group and five –S– ligands.

DISCUSSION

Ferricyanide-oxidized nitrate reductase

The EXAFS data on the ferricyanide-oxidized enzyme strongly suggest the presence of two =O ligands to Mo(VI) of the *T. pantotropha* periplasmic nitrate reductase. This contrasts with the uniquely low apparent =O content of the oxidized *Escherichia coli* membrane-bound respiratory nitrate reductase of 0.5–1.0 [25,26] and further highlights the differences between the molybdenum centres of the membrane-bound and periplasmic enzymes previously suggested by EPR [16] and analysis of the primary protein structures [17] .

The EXAFS also suggests the presence of at least three –S– ligands. The exclusion of chloride from the ferricyanide-oxidized enzyme rules out the possibility that a –Cl ligand could be mistaken for an –S–. A sixth ligand could be –O–, –N– or –S–, but the EPR data [16] preclude –OH and –SH and argue against –N– on the basis of the absence of a ^{14}N (I=1) superhyperfine interaction with Mo(V) [18].

Assuming that two of the Mo –S– groups are due to the dithiolene moiety of the cofactor, possible sources for a –O– and two –S– ligands need to be considered. A cysteine conserved in the assimilatory and periplasmic nitrate reductases (Cys-181 in the periplasmic nitrate reductase of *T. pantotropha*) (Figure 4) and conserved as Cys or selenoCys in the formate dehydrogenases is a strong candidate for a third –S– ligand [7,16,17] (see below). A second cysteine 21 residues downstream of the first, which is conserved in the periplasmic nitrate reductases (Figure 4), is a candidate for a fourth –S– ligand. Alternatively, a non-hydroxyl Mo –O– ligand could be due to a conserved serine residue three residues after the first conserved cysteine (Figure 4).

Dithionite-reduced nitrate reductase

Although > 95% of the molydenum in the dithionite-reduced nitrate reductase samples was Mo(IV), we cannot be certain that there were not two Mo(IV) states, since EPR analysis of the small amount (< 5%) of Mo(V) in the dithionite-reduced sample revealed the presence of both High-*g* Split and Pseudo Rapid Unsplit signals. The relative amounts of the Mo(IV) analogues of these species is, however, unknown. If, as is proposed [16,19], the origin of the Pseudo Rapid Unsplit species is related to reduction of the pterin of the molybdenum cofactor, then the amounts of the Mo(IV) analogues of each of the Mo(V) EPR-signal-giving species would depend on the extent of reduction. Dithionite is a strong enough reductant to reduce essentially all of the molybdenum to Mo(IV) and would be expected to favour the production of a Pseudo Rapid Mo(IV) analogue.

Analysis of the EXAFS data on the dithionite-reduced nitrate reductase indicates that the species contains one =O group and

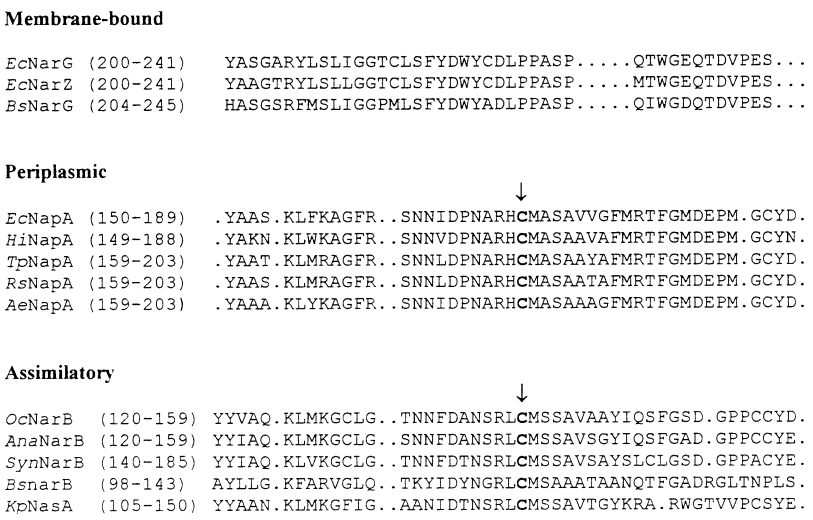

Figure 4 Alignment of the segment 3 [7] regions of the membrane-bound, periplasmic and assimilatory nitrate reductases

*Ec*NarG, *E. coli* membrane-bound nitrate reductase A [30]; *Ec*NarZ, *E. coli* membrane-bound nitrate reductase Z [31]; *Bs*NarG, *Bacillus subtilis* membrane-bound nitrate reductase [28]; *Ec*NapA, *E. coli* periplasmic nitrate reductase [32]; *Tp*NapA, *T. pantotropha* periplasmic nitrate reductase [17]; *Hi*NapA, *Haemophilus influenza* periplasmic nitrate reductase [33]; *Rs*NapA, *Rhodobacter sphaeroides* periplasmic nitrate reductase [34]; *Ae*NapA, *Alcaligenes eutrophus* periplasmic nitrate reductase [35]; *Syn*NarB, *Synechococcus* species PCC7942 assimilatory nitrate reductase [36]; *Oc*NarB, *Oscillatoria chalybea* asimilatory nitrate reductase [37]; *Ana*NarB, *Anabaena* sp. assimilatory nitrate reductase [38]; *Kp*NasA, *Klebsiella pneumoniae* assimilatory nitrate reductase [39]; *Bs*NarB, *B. subtilis* assimilatory nitrate reductase [40]. Residue positions are shown in parentheses. The arrow indicates the position of the conserved Cys-181.

four –S–/–Cl. No sample was analysed in the absence of chloride. The EPR of the High-*g* Split Mo(V) shows no anion effects, but generation of the low-potential Pseudo Rapid EPR signal is pH dependent and could be anion or buffer dependent [16]. Thus it cannot be excluded that at least one species of the reduced [Mo(IV)] enzyme does indeed bind a chloride ligand. As with the oxidized enzyme, the possibility of there being an Mo –O– ligand arises. The nature of such a ligand is difficult to predict. The high Debye–Waller factor calculated for the Mo –S–/–Cl ligands may be a manifestation of some geometrical inhomogeneity of the molybdenum centres in the sample.

Implications from EXAFS of Mo(VI)- and Mo(IV)-containing nitrate reductase regarding the Mo(V) species of the enzyme

Since the EXAFS suggests the presence of only two oxo ligands in the Mo(VI) state and one oxo ligand in the Mo(IV) state(s), it is possible that reduction of Mo(VI) to Mo(V) is accompanied by reduction of one of the =O ligands to –O–. All of the Mo(V) species of the enzyme characterized thus far by EPR are available as proportions of the total molybdenum content of only up to $\sim$ 30% [16]. Therefore the Mo(V) state of the enzyme is not amenable to direct EXAFS analysis. However, since the nitrate-treated nitrate reductase sample contained around 30% Mo(V) and 70% Mo(VI), analysis of the EXAFS of this sample can be used to infer the structure of the Mo(V) ion. The optimum fit of the EXAFS data on the nitrate-treated enzyme included 1.8 oxo ligands. Assuming that the =O content of the 70% Mo(VI) is two, this non-stoichiometric figure could be accounted for if the =O content of the 30% Mo(V) species in this sample is one, consistent with the scheme of reduction outlined above.

In desulpho xanthine oxidase and related enzymes the result of reduction of Mo=O is Mo–OH in which the proton, which is readily exchangeable with solvent-derived ^{2}H, is clearly identifiable due to its large superhyperfine splitting of the EPR spectrum [27]. Such a proton does not exist in the High-*g* Split Mo(V) species of soluble nitrate reductases [16,18]. In other Mo(V) oxomolybdenum enzyme species where such a proton does not exist, such as the *E. coli* membrane-bound nitrate reductase High-pH species, ligand replacement by added anions or buffer ions has been shown to occur (e.g. [26]). With the soluble nitrate reductases anion binding has been sought but not found [16]. Thus the putative –O– ligand of the periplasmic nitrate reductase Mo(V) appears not to be protonated. It is possible that an anionic form, Mo–O$^-$, is present that could be stabilized by hydrogen bonding to one or more electrophilic species. Alternatively ligand exchange could occur upon reduction of one of the EXAFS-identified Mo(VI)=O groups in which the resulting Mo–OH was exchanged with, for instance, serine –O–, cysteine –S– or perhaps cofactor ribose 2′- or 3′-hydroxyl groups. Two non-exchangeable protons are seen in the EPR spectrum of the Mo(V) High-*g* Split species of *T. pantotropha* nitrate reductase, both weakly coupled with $A(^1\mathrm{H})$ of ~ 0.5 and ~ 0.2 mT [16]. However, for serine or cysteine ligands the C protons would be expected to be identical (provided that rotation around a single bond were not prevented for steric reasons) and therefore would not be expected to display the disparity in $A(^1\mathrm{H})$ observed.

Implications for Mo co-ordination in the periplasmic, assimilatory and membrane-bound nitrate reductases

The EXAFS of the periplasmic nitrate reductase has strongly suggested the presence of two =O ligands to Mo(VI) and one to Mo(IV). This clearly distinguishes the molybdenum site of the periplasmic nitrate reductase from that of the membrane-bound enzyme which has 1 =O ligand in the Mo(VI) Low-pH form and 0.5 =O ligand (possibly zero) in the Mo(IV) Low-pH form [26]. The Mo(VI) of the periplasmic and Low-pH membrane-bound nitrate reductases have three/four –S– ligands and four –S– ligands respectively (this work and [26]). We suggest that the

origin of these –S– ligands is different. In the periplasmic nitrate reductase Cys-181 (*T. pantotropha* numbering) is conserved in the segment 3 region proposed to form part of the Mo-binding site (Figure 4) [7,17]. This is also conserved as Cys or selenoCys in the MGD-dependent formate dehdrogenases [7]. EPR has clearly established that the Se of SeCys is an Mo ligand [29]. Therefore it is likely that the conserved Cys residue in the formate dehdrogenases and periplasmic nitrate reductases is also a Mo ligand. The presence of an Mo–S–Cys ligand in the periplasmic nitrate reductase has been invoked to explain the EPR signals of the enzyme [16]. Thus we suggest that three of the Mo(VI) –S– ligands arise from the pterin–pyran dithiolene and Cys-181. Cys-181 is also conserved in the bacterial cytoplasmic assimilatory nitrate reductases (Figure 4). Comparison of the EPR signals from *T. pantotropha* periplasmic nitrate reductase and *Azotobacter vinelandii* assimilatory nitrate reductase suggest very similar co-ordination spheres [16,18]. There is no conserved equivalent to Cys-181 in the membrane-bound nitrate reductase (Figure 4). In some previous alignments of the segment 3 region of MGD enzymes, Cys-222 (*E. coli* NarG numbering) has been aligned with the the conserved Cys/SeCys (e.g. [29]). However, the segment 3 region of the membrane-bound nitrate reductases has very poor sequence similarity with the periplasmic and assimilatory enzymes, and consideration of the recently published sequence from *Bacillus subtilis* [28] reveals that Cys-222 is not conserved (Figure 4). The tungstopterin aldehyde oxidase of *Pyrococcus furiosis* is liganded by the dithiolenes of two pterin–pyran cofactors, raising the possibility that dipterin ligation could also be present in the nitrate reductases [6]. Assuming that a cysteine –S– ligand is present, dipterin ligation (i.e. a total of five –S–) can be excluded for the periplasmic nitrate reductase because of the extremely poor fit of the EXAFS to more than four –S–. However, for the membrane-bound nitrate reductase, in the absence of a candidate cysteine –S–molybdenum ligand, four –S– ligands arising from dipterin ligation should still be considered.

We wish to thank A. Reilly for assistance in enzyme preparation of the enzyme and M. Hart for the molybdenum analyses. This research was supported by DRAL (EPSRC) grant 25/108 to C.D.G., J.C.C., B.B., B.C.B., D.J.R., E.M. Armstrong and A. Dinsmore and grant 83/C02012 from the BBSRC to D.J.R. and S.J.F.

REFERENCES

1 Coughlan, M. P. (1980) Molybdenum and Molybdenum-Containing Enzymes, Pergamon Press, Oxford
2 Burgess, B. K. (1990) Chem. Rev. **90**, 1377–1406
3 Kim, J. and Rees, D. C. (1992) Science **257**, 1677–1682
4 Rajagopalan, K. V. and Johnson, J. L. (1992) J. Biol. Chem. **267**, 10199–10202
5 Romão, M. J., Archer, M., Moura, I., Moura, J. J. G., LeGall, J., Engh, R., Schneider, M., Hof, P. and Huber, R. (1995) Science **270**, 1170–1176
6 Chan, M. K., Swarnalatha, M., Kletzin, A., Adams, M. W. W. and Rees, D. C. (1995) Science **267**, 1463–1469
7 Berks, B. C., Ferguson, S. J., Moir, J. W. B. and Richardson, D. J. (1995) Biochim. Biophys. Acta. **1232**, 97–173
8 Vincent, S. P. and Bray, R. C. (1978) Biochem. J. **171**, 639–647
9 Adams, M. W. W. and Mortenson, L. E. (1985) in Molybdenum Enzymes (Spiro, T. G., ed.), pp. 519–593, Wiley Interscience, New York
10 Morpeth, F. F. and Boxer, D. H. (1985) Biochemistry **24**, 40–46
11 Turner, N. A., Ballard, A. L., Bray, R. C. and Ferguson, S. J. (1988) Biochem. J. **282**, 925–926
12 Guigliarelli, B., Asso, M., More, C., Augier, V., Blasco, F., Pommier, J., Giordano, G. and Bertrand, P. (1992) Eur. J. Biochem. **207**, 61–71
13 Berks, B. C., Berks, B. C., Page, M. D., Reilly, A., Richardson, D. J., Outen, F. and Ferguson, S. J. (1995) Mol. Microbiol. **15**, 319–331
14 Berks, B. C., Richardson, D. J., Robinson, C., Reilly, A., Aplin, R. T. and Ferguson, S. J. (1994) Eur. J. Biochem. **220**, 117–124
15 Breton, J., Berks, B. C., Reilly, A., Thomson, A. J., Ferguson, S. J. and Richardson, D. J. (1994) FEBS Lett. **345**, 76–80
16 Bennett, B., Berks, B. C., Ferguson, S. J., Thomson, A. J. and Richardson, D. J. (1994) Eur. J. Biochem. **226**, 789–798
17 Berks, B. C., Richardson, D. J., Reilly, A., Willis, A. C. and Ferguson, S. J. (1995) Biochem. J. **309**, 983–992
18 Gangeswaran, R., Lowe, D. J. and Eady, R. R. (1993) Biochem. J. **289**, 335–342
19 Sears, H. J., Bennett, B., Spiro, S., Thomson, A. J. and Richardson, D. J. (1995) Biochem. J. **310**, 311–314
20 Bell, L. C., Page, M. D., Berks, B. C., Richardson, D. J. and Ferguson, S. J. (1993) J. Gen. Microbiol. **139**, 3205–3214
21 Binsted, N., Campbell, J., Gurman, S. J. and Stephenson, P. C. (1991) SERC Daresbury Laboratory EXCURV92 program
22 Lee, P. A. and Pendry, J. B. (1975) Phys. Rev. **B11**, 2795–2811
23 Gurman, S. J., Binsted, N. and Ross, I. (1984) J. Phys. **C17**, 143–151
24 Hedin, L. and Lundqvist, S. (1969) Solid State Phys. **23**, 1–181
25 Cramer, S. P., Solomonson, L. P., Adams, M. W. W. and Mortenson, L. E. (1984) J. Am. Chem. Soc. **106**, 1467–1471
26 George, G. N., Turner, N. A., Bray, R. C., Morpeth, F. F., Boxer, D. H. and Cramer, S. P. (1989) Biochem. J. **259**, 693–700
27 Bray, R. C. (1988) Q. Rev. Biophys. **21**, 299–329
28 Ramos, H. C., Boursier, L., Moszer, I., Kunst, F., Danchin, A. and Glaser, P. (1995) EMBO J. **14**, 5984–5994
29 Gladyshev, V. N., Khangulov, S. V., Axley, M. J. and Stadtman, T. C. (1994) Proc. Natl. Acad. Sci. U.S.A. **91**, 7708–7711
30 Blasco, F., Giordano, G., Chippaux, M. and Bonnefoy, V. (1989) Mol. Gen. Genet. **218**, 249–256
31 Blasco, F., Iobbi, C., Ratouchniack, J., Bonnefoy, V. and Chippaux, M. (1990) Mol. Gen. Genet. **222**,104–111
32 Richterich, P., Lakey, N., Gryan, G. et al. (1993) Accession number U00008, EMBL Nucleotide Sequence Database, Heidelberg
33 Fleischmann, R. D., Adams, M. D., White, O. et al. (1995) Science **269**, 496–512
34 Reyes, F., Rioldan, M. D., Klipp, W., Castillo, F. and Moreno-Vivian, C. (1996) Mol. Microbiol. **19**, 1307–1318
35 Siddiqui, R. A., Warnecke-Ebertz, U., Hengsberger, A., Schnieder, B., Kostka, S. and Friedrich, B. (1993) J. Bacteriol. **175**, 5867–5876
36 Andriesse, A. J. and Bakker, H. (1993) Accession number X74597, EMBL Nucleotide Sequence Database, Heidelberg
37 Unthan, M., Klipp, W. and Schmid, G. H. (1995) Accession number X89445, EMBL Nucleotide Sequence Database, Heidelberg
38 Cai, Y. and Wolk, C. P. (1995) Accession number L49163, EMBL Nucleotide Sequence Database, Heidelberg
39 Lin, J. T., Goldman, B. S. and Stewart, V. (1993) J. Bacteriol. **175**, 2370–2378
40 Ogawa, K. I., Nakano, M. M., Zubar, P. and Yamane, K. (1995) Accession number D30689, EMBL Nucleotide Sequence Database, Heidelberg

Received 7 February 1996; accepted 25 March 1996